

# RING-SHAPED N<sup>+</sup>/P-WELL PHOTODIODE: STUDY OF RESPONSIVITY ENHANCEMENT

*Tatiana Danov, Igor Shcherback, Orly Yadid-Pecht, Senior Member, IEEE*

The VLSI Systems Center  
Ben Gurion University  
P.O.B. 653 Beer-Sheva 84105, ISRAEL  
Tel: 972-8-646152; Fax: 972-8-6477620  
E-Mail: oyp@ee.bgu.ac.il

## ABSTRACT

In this work the possibilities of CMOS APS spectral response improvement is discussed. Thorough submicron scanning results obtained from various ring-shaped pixel photodiodes with different inner radius, implemented in a standard CMOS 0.35 $\mu$ m technology, are compared with numerical computer simulations. The functional dependence of the pixel response on the ring opening size was discovered and formulated for various wavelengths illumination. We show that the photodiodes with small ring-opening exhibit better sensitivity in the blue spectrum range (420-460 nm). Comparison between the simulation and measurement results shows a good agreement and, therefore, involving specific photodiode enables to improve the pixel color selectivity design.

**Index Terms** - APS (Active Pixel Sensor), CMOS image sensor, minority carriers, diffusion, photocurrent, sensitivity.

## 1. INTRODUCTION

Nowadays, CMOS based imagers offer significant advantages over CCD's such as a low voltage, low power consumption, lower cost [1]. In the time of CMOS technology rapid downscale, small pixel size, low dark current, high fill factor, and low noise are required for the high resolution imagers. The achievement of the sensitivity from the available CMOS structures, comparable to these of CCDs, is still one of the major manufacturers problems. Various specialized devices and materials have been developed to increase the sensitivity without costing too much in pixel area [2]-[5]. An analysis of the pixel design effect on the APS responsivity was performed in [6]-[8]. In this paper, we investigate the influence of the ring-shaped photodiode design on APS sensitivity, and show the ensuing enhancement of the device sensitivity to short wavelengths illumination, i.e. to blue light. The opto-electrical characteristics of the ring-structures are described in Sections 2-3.

## 2. SIMULATION RESULTS

### 2.1 Background

Photon absorption in the silicon depends on the wavelength dependant absorption coefficient  $\alpha(\lambda)$ . The collection of the photogenerated carriers depends on the carrier absorption depth,  $L_{opt}=1/\alpha$ , lifetime ( $\tau_n$  or  $\tau_p$ ), and the characteristic diffusion length ( $L_n$  or  $L_p$ ). Perfect collection efficiency is assumed for the electron-hole pairs generated within the device depletion region. Carriers generated outside the depletion region may be collected as they might diffuse into the depletion region.

Red light, with wavelength,  $\lambda\sim 0.6\mu$ m for instance, have relatively small absorption coefficient, which means more of the photocarriers can be generated outside the depletion region (p-type substrate in our case). These carriers diffuse to the original imaging site or to a nearby site where they are collected, before they are lost to a bulk recombination process. The imagers lose resolution as the result of this diffusion process.

Blue photons,  $\lambda\sim 0.4\mu$ m, tend to be absorbed near the device surface (into the N<sup>+</sup> region in our case). The high doping density in this region strongly reduces the carrier lifetime, such that most of the minority carriers recombine immediately; causing therefore low photodiode sensitivity for short wavelengths illumination.

### 2.2 Simulation of the Opto-Electrical Characteristics

We have investigated the photoresponse in CMOS ring-shaped photodiodes by means of numerical device simulations for different wavelength illuminations (covering the visible spectrum, 420-700 nm). The simulator used is called *Medici*<sup>TM</sup> [9] and it solves the Poisson's and continuity equations. Ring-shaped N<sup>+</sup>/P-Well photosensitive elements with different inner-ring-radiuses (i.e., 0.2  $\mu$ m, 0.25  $\mu$ m, 0.35  $\mu$ m, 0.5  $\mu$ m, and 0.6  $\mu$ m) were investigated. Note that all the simulations are based on the parameters reported for the standard CMOS 0.35- $\mu$ m technology process. The simulation results are compared with the results obtained by thorough scanning of various ring-shaped photodiode APS fabricated in standard 0.35 $\mu$ m CMOS technology. Note that the

illumination spot size and photon flux kept constant (for each  $\lambda$ ) in order to simplify the results comparison.

Fig.1 shows the normalized output signal distribution obtained from different inner-radius photodiodes as a function of the illuminating spot position. It is possible to see that the photosignal from the ring-opening decreases as the ring-radius increases (the normalized photosignal varies from 0.67 for  $r_{inner}=0.6 \mu m$ , to 0.97 for  $r_{inner}=0.2 \mu m$ ), while the signal magnitude from the active-ring part remains unaltered (the normalized photosignal is  $\approx 1$ ).

Fig.2 presents an example of the normalized photosignal versus light spot position, obtained for the particular photodiode (with  $r_{inner}=0.25 \mu m$ ), and different wavelengths. The diode reveals the intensified response in the blue region (420-460 nm), i.e., the photosignal from the ring-opening region is higher than one from the active part of the diode.

Fig.3 represents the simulation results obtained for several ring photodiodes in blue spectral diapason. The photoresponse obtained from ring-opening is compared with the corresponding active-part response (the  $N^+$  part photoresponse, which is indicated by the dashed line). It is possible to see that the diodes with small opening-radius exhibit higher sensitivity in comparison to diodes illuminated in active area, i.e., the "blue" signal from the "window" stays higher than the "blue" signal from the ring itself, in all range from 420 nm to 460 nm. Note that the "window" dominance reduces with wavelength increase, such that the difference between "window" and ring-part signals varies from 4% for 420 nm to 2 % for 460 nm.

### 3. COMPARISON WITH EXPERIMENTAL RESULTS AND DISCUSSION

In order to check the presented simulation results we have performed experimental investigations by means of a unique sub-micron scanning system (S-cube system) [10]- [11], that enables a detailed, point by point, quantitative determination of the contributions to the total output signal from each particular region of the pixel. A set of various ring-shaped  $7 \mu m$ -pitch pixels (see Fig. 4 for the layout example) fabricated in standard CMOS  $0.35 \mu m$  technology was thoroughly scanned in several wavelengths illumination.

Fig. 5 shows the exemplifying responsivity map obtained for  $\lambda=454nm$  by thorough sub-micron scanning for a ring-shaped pixel illustrated in Fig. 4.

Two lines in Fig.6 corroborate the simulation results and present the averaged responsivity maps cross-section through the photodiode center for  $\lambda=454nm$  (the solid line at Fig.6) and  $\lambda=632nm$  (the dashed line at Fig.6) corresponding to

Figs. 4 and 5. In Fig. 6 the response for  $\lambda=632nm$  is "flat", while for  $\lambda=454nm$  the photosignal from the "window" region (region "A") is higher than in the active part (regions "B" and "C", where the difference between "blue" signals from regions "A" and "B" or "C" is estimated to be 16%).

It is possible to understand and explain this effect with regard to the absorption mechanism in silicon.

The absorption depth for "blue" photons is a few tenths of micrometers, i.e., most of the potential contributors created close to the surface and should be absorbed before they lost in recombination. The ring-shaped photodiode architecture evolved mainly from this basic requirement: the depletion region (which has two collection areas: bottom and sidewall collection areas [8]) should be spaced closely to the surface. The peculiarity of the silicon interaction with the blue light allows to assert that the sidewall collection area of the depletion region becomes dominant for "blue" photocarriers collection. Moreover, keeping in mind the scaling tendencies, i.e., the shallower depletion and highly doped regions, this requirement becomes more significant [12].

The ring photodiode architecture enables its sidewall collection region enlargement. Blue photocarriers created within the ring-opening diffusing quickly towards the very closely set sidewall depletion, since they are surrounded by a sidewall of the space charge region. Moreover, the photocarrier creation can occur within the depletion sidewall itself and directly contribute the signal. The schematic illustration of this process is shown on Fig.7. Therefore, the excess "blue" carriers loss decreases, the photoelectron collection efficiency of the photodiode increases, and pixel electrical signal increases. Note that most of the "red" contributors are collected through the bottom depletion collecting surface, since they are generated in the deep substrate (5-8  $\mu m$ ) and then diffuse in all directions.

### 4. CONCLUSIONS

In this work, an investigation of a ring-shaped photodiode CMOS APS has been presented. The simulation and experimental results obtained from different inner-radius photodiodes present pixel sensitivity improvement in "blue" spectral region. This property of pixel photodiode was discovered in diodes with a relatively small opening size, clearing therefore the way for further investigation in more advanced CMOS technologies. Moreover, the presented results determine the line for further improve and "intelligent" design optimization, enabling required optical response and desirable color differentiation.

## 5. REFERENCES

- [1] O. Yadid-Pecht, "CMOS Imagers course notes," Ben Gurion University, 2000.
- [2] B. C. Burkley *et al.*, "The pinned photodiode for an interline-transfer CCD image sensor," in *IEDM Tech. Dig.*, pp.28, 1984.
- [3] S. Manabe *et al.*, "A 2-million-pixel CCD image sensor overlaid with an amorphous Silicon photoconversion layer," *IEEE Trans. Electron Devices*, vol. 38, pp.1765, Aug. 1991.
- [4] S. Mendis, S. Kemeny, and E.R. Fossum, "A 128x128 CMOS active pixel image sensor for highly integrated imaging systems," in *IEDM Tech. Dig.*, pp. 583, 1993.
- [5] T. Lule S. Benthien, H. Keller, et al., "Sensitivity of CMOS Based Imagers and Scalling Perspectives," *IEEE Trans. Electron Devices*, vol. 47, pp.2107-2122, Nov. 2000.
- [6] O. Yadid-Pecht, B. Mansoorian, E. Fossum, B. Pain, "Optimization of active pixel sensor noise and responsivity for scientific applications", *Proc. SPIE/IS&T Sym. on Electronic Imaging: Science and Technology*, San Jose, California, Feb 10-13, 1997.
- [7] J. S. Lee, R. I. Hornsey, "CMOS Photodiodes with Substrate Openings for Higher Conversion Gain in Active Pixel Sensors," *2001 IEEE Workshop on CCDs and Advanced Image Sensors*, Crystal Bay, Nevada, June 2001.
- [8] I. Shcherback and O. Yadid-Pecht, Chapter 3, in "CMOS IMAGERS: FROM PHOTOTRANSDUCTION TO IMAGE PROCESSING," O. Yadid-Pecht and Ralph Etienne-Cummings (Eds.), Kluwer academic publishers, spring 2004.
- [9] Avant! Corporation, Medici 4.1 User's Manual, Fremont, CA, July 1998.
- [10] I. Shcherback, O. Yadid-Pecht, "CMOS APS Crosstalk Characterization Via a Unique Submicron Scanning System," *IEEE Trans. Electron Devices*, Vol. 50, No. 9, pp.1994-1997, Sept. 2003.
- [11] I. Shcherback, B. Belotserkovsky, O. Yadid-Pecht, "A Unique Sub-micron Scanning System use for CMOS APS crosstalk characterization," in *Proc. SPIE on Sensors, Cameras and Systems for Scientific/Industrial Applications*, San Jose, California USA, 22-23 January, 2003.
- [12] I. Shcherback, O. Yadid-Pecht, "Prediction of CMOS APS Design Enabling Maximum Photoresponse for Scalable CMOS Technologies," *IEEE Trans. Electron Devices*, Vol. 51, No. 2, pp. 279- 282, Feb. 2004.

### List of Figures

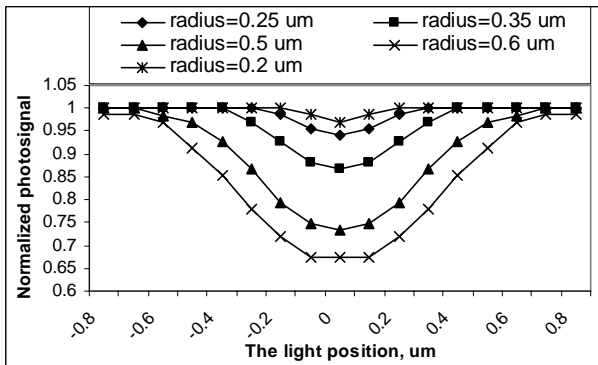


Fig. 1: The normalized output signal distribution obtained from different inner-radius photodiodes as a function of the illuminating spot position ( $\lambda=632\text{nm}$ ). The point of  $0\ \mu\text{m}$  corresponds to the ring center of the photodiode.

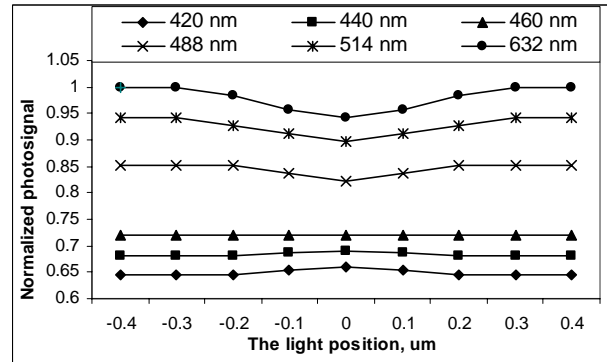


Fig. 2: Example of the normalized electrical signal simulated for the diode with inner radius of  $0.25\ \mu\text{m}$ . The characteristics obtained in the visible range (420-460 nm). The point of  $0\ \mu\text{m}$  corresponds to the ring center of the photodiode.

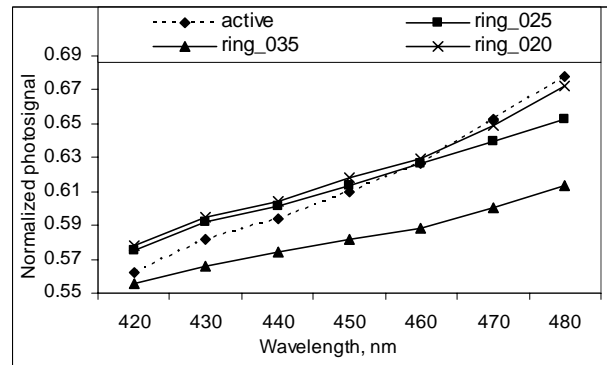


Fig. 3: The pixel sensitivity characteristics, simulated for several ring photodiodes (with a small inner radius), in blue spectral diapason. The dashed line demonstrates the photosignal corresponding to the diode illumination directed towards the active part (the N+ region); the solid lines correspond to the "window" lighting (P-Well region).

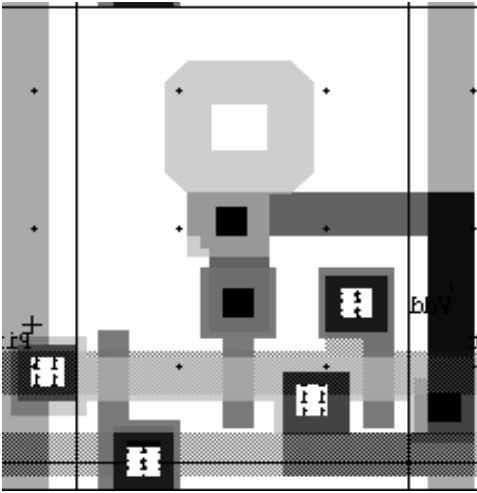


Fig. 4: The design layout example of ring-shaped active area pixel with inner photodiode radius of 0.4  $\mu\text{m}$ , and active layer (ring) width of 0.6  $\mu\text{m}$ .

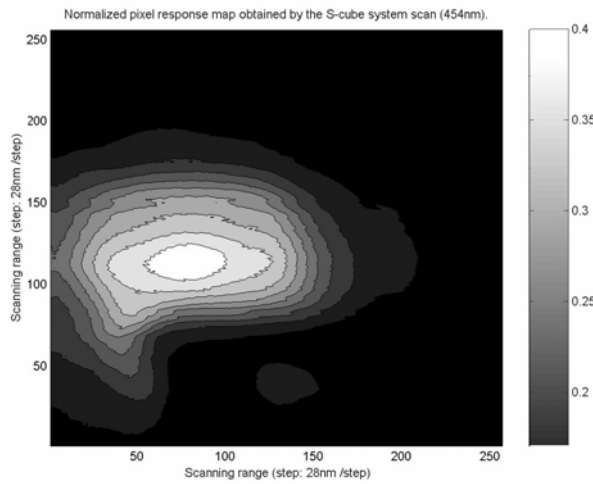


Fig. 5: The pixel normalized response map example obtained by the S-cube system scan (454 nm) in correspondence to Fig. 4.

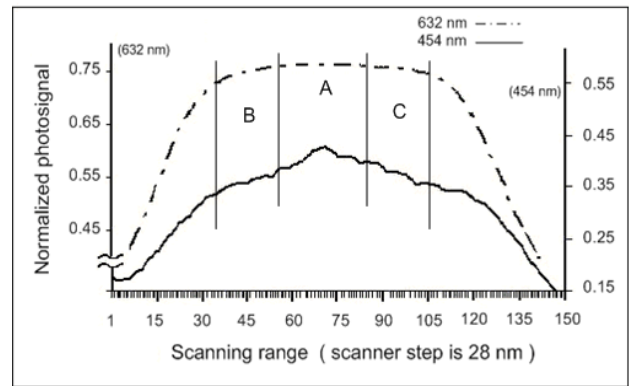


Fig. 6: The averaged responsivity maps cross-section through the photodiode center for  $\lambda=454\text{nm}$  (the solid line) and  $\lambda=632\text{nm}$  (the dashed line) corresponding to Figs. 4 and 5. The response for  $\lambda=632\text{nm}$  is “flat”, while for  $\lambda=454\text{nm}$  the photosignal from the “window” region (region “A”) is higher than in the active part (regions “B” and “C”), where the difference between “blue” signals from regions “A” and “B” or “C” is estimated to be 16%.

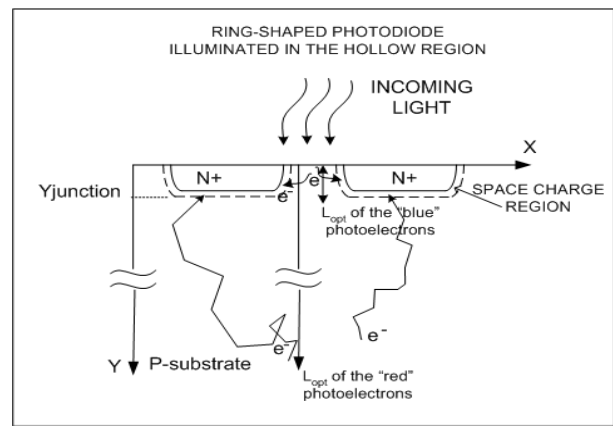


Fig. 7: Schematic cross section of the the ring-diode through its center. The difference between the “blue” and the “red” photons absorption mechanisms is indicated regarding different absorption depths, i.e.,  $L_{opt}^{red} \gg L_{opt}^{blue}$ .